



Scholars Research Library

Der Pharma Chemica, 2014, 6(4):398-405
(<http://derpharmachemica.com/archive.html>)



ISSN 0975-413X
CODEN (USA): PCHHAX

Mechanism of interaction of antibacterial drug moxifloxacin with herring sperm DNA: Electrochemical and spectroscopic studies

Mallappa M¹, Babu G Gowda^{1*} and R T Mahesh²

¹Department of Chemistry, Maharani's Science College for Women, Bangalore, India

²R & D Division, Kemwell Biopharma Pvt. Ltd., Nelamangala, Bangalore, India

ABSTRACT

The interaction between Moxifloxacin (MXF) and Herring Sperm DNA (Hs-DNA) was investigated by using voltammetric (CV and DPV), UV-vis, spectrofluorometric and viscometric methods in Britton-Robinson (BR) buffer of pH 7.4. The binding of MXF to Hs-DNA was substantiated by the hypochromism and bathochromism in the absorption and the emission quenching in fluorescence spectra. The voltammetric method using carbon paste electrode (CPE) suggested an electrostatic interaction, while spectroscopic methods show minor groove binding as the predominant mode. The values of binding constants obtained from UV absorption, spectrofluorimetry and voltammetric measurements were in close agreement. The obtained results confirmed that the present method is a good alternative for the determination of the binding constant and site number for the molecular interaction.

Keywords: Moxifloxacin, Herring Sperm DNA, voltammetry, Spectroscopy, Binding constant

INTRODUCTION

Moxifloxacin (MXF) (Fig. 1) is a fourth-generation fluoroquinolone antibacterial agent active against a broad spectrum of Gram-positive and Gram-negative ocular pathogens, a typical microorganisms and anaerobes [1]. It differs from the other quinolones by having a methoxy radical at the 8-position, with an S, S-configured diazabicyclonoyl ring moiety at the 7-position, and by having improved anti-bacterial activity over other similar quinolones [2-4]. Moreover, this compound appears to cover bacterial resistance to second- and third-generation fluoroquinolones [5,6].

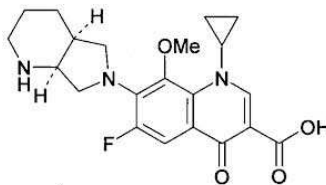


Fig 1: Structure of Moxifloxacin

DNA is known to be a major target for drugs and some harmful chemicals to be attacked. Small molecules normally interact with DNA via non covalent interaction modes. Therefore, the study of the possible interactions of the drug with endogenous compounds is important. The interaction between drugs and DNA is a fundamental issue in life process, and it is crucial for gene therapy due to correlation with the mechanisms of drug and gene delivery systems. Intercalation, groove binding, and electrostatic interactions are the three major binding modes of small molecules to DNA [7].

So far, the studies on the interaction between MXF and Hs-DNA have not been reported in the literature. In this work, the interaction of MXF with herring sperm DNA (Hs-DNA) is investigated using voltammetry, spectroscopic and viscometric techniques. The binding constant of MXF to DNA was calculated and the binding mechanism is discussed. We hope the results obtained in this work will provide some additional useful information for the evaluation of the safety performance of MXF through understanding their interaction with DNA.

MATERIALS AND METHODS

1.1. Apparatus

Electrochemical experiments were performed in a conventional three-electrode cell powered by an electrochemical system comprising Analyzer model-201 system. A carbon paste electrode (CPE) was used as working electrode, a platinum wire as a counter electrode and a calomel electrode as reference electrode.

The UV-vis spectra were recorded on a double beam Ellico UV-visible spectrophotometer (INDIA) in matched quartz cell of 1-cm path length. The fluorescence measurements were carried out on a HITACHI F-4500 spectrofluorimeter equipped with a 150W Xenon lamp and 1-cm quartz cell. The titrations were performed by keeping the constant of MXF concentration and varying concentration of Hs-DNA. The pH measurements were made with Scott Gerate pH meter CG 804. An electronic thermostat water-bath was used for controlling the temperature.

1.2. Reagents

Hs-DNA with a purity of > 98 %, MXF with a purity of > 99% and all other chemicals were purchased from Sigma Aldrich (India). They were used without further purification. The solutions were stored at 4°C before being used. Britton-Robinson (BR) buffer pH 7.4 was prepared by following the standard methods and was used as a supporting electrolyte. Analytical grade reagents and double distilled water were used throughout the experiment.

RESULTS AND DISCUSSION

3.1. Electrochemical Oxidation of MXF

The electrochemical behaviour of MXF at CPE was investigated employing CV and DPV. Among various supporting electrolytes, MXF (1.0×10^{-5} M) showed higher signal response in BR buffer of pH 7.4. MXF showed an anodic peak at -981 mV in BR buffer of pH 7.4 with scan rate of 50 mVs^{-1} . No peak was observed in the reverse scan but when the scan rate is increased, the peak potential shifted to negative values suggesting that the oxidation of MXF at CPE is irreversible [Fig. 2].

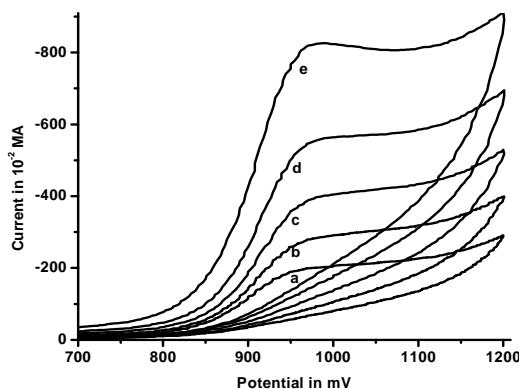
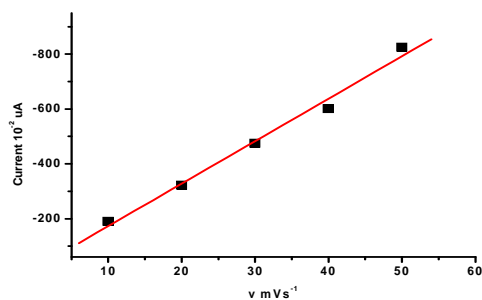
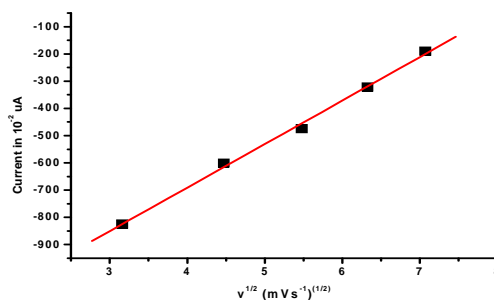


Fig 2: Cyclic voltammogram of MXF on CPE Supporting electrolyte: BR buffer (pH 7.4); (a) 10 mVs^{-1} ; (b) 20 mVs^{-1} ; (c) 30 mVs^{-1} ; (d) 40 mVs^{-1} and (e) 50 mVs^{-1}

The plots of $\log I_p$ vs $\log v$ in the scan rate range of 10 - 50 mV s^{-1} yielded a straight line with slope of 0.8934. This value is close to the theoretical value, 1.00, which is expected for an ideal reaction condition for adsorption controlled electrode process [8,9]. The graph obtained has good linearity between I_{pa} vs scan rate (v) ($R^2 = 0.9943$) and I_{pa} vs $v^{1/2}$ ($R^2 = 0.9985$) [Fig. 3 A & B].

Fig 3A: Graph of I_{pa} vs. v of MXFFig 3B: Graph of I_{pa} vs. $v^{1/2}$ of MXF. Supporting electrolyte: BR buffer (pH 7.4).

In the range from 10 to 50 mV s^{-1} the anodic peak currents were proportional to the scan rate which indicates, the electrode reaction was adsorption controlled [9]. Hence, the electrooxidation of MXF involves the transfer one electron [10]. The probable reaction mechanism of electrooxidation of MXF was shown in Fig. 4. [10,11].

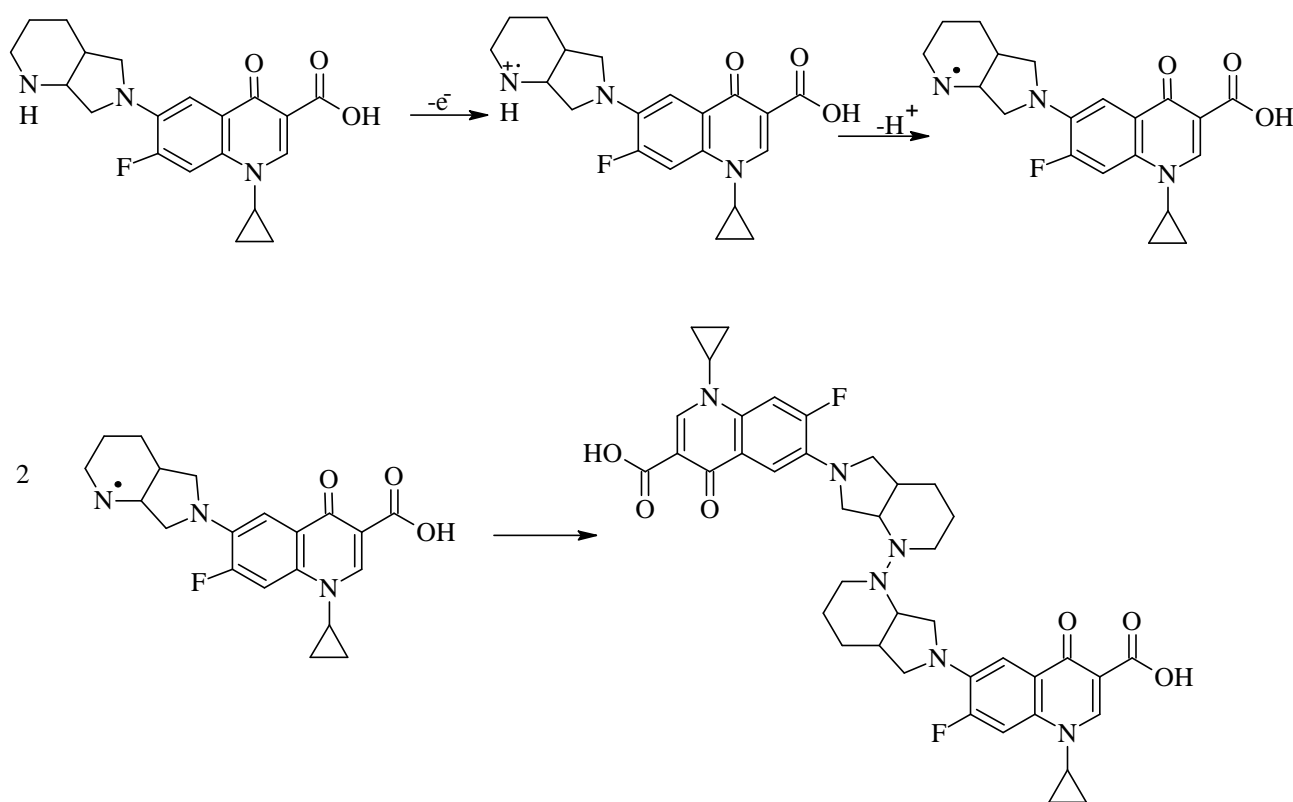


Fig 4: Probable mechanism for electrooxidation of MXF

The electron transfer coefficient ' α ' is calculated from the difference between peak potential (E_p) and half wave potential ($E_{p/2}$) according to equation given below [12]:

$$\Delta E_p = E_p - E_{p/2} = (47.7/\alpha) \text{ mV (irreversible reaction; at 298 K)}$$

The obtained value of α is 0.539. For an irreversible oxidation reaction, we may use the following equation to calculate standard rate constant (k_0) [13,14].

$$E_p = E^0 + (RT/\alpha n) [\ln (RTk_0/\alpha nF) - \ln v]$$

Where E_0 is the formal potential, R was the universal gas constant ($8.314 \text{ J K}^{-1} \text{ mol}^{-1}$), T (K) was the Kelvin temperature, α was the transfer coefficient, k_0 (s^{-1}) was the electrochemical rate constant and F was the Faraday constant ($96,487 \text{ C mol}^{-1}$). The value of E^0 was obtained from the intercept of the E_p vs v plot by the extrapolation to the vertical axis at $v = 0$. The value of k_0 were evaluated from the plot of E_p vs $\ln v$ and found to be $0.9849 \times 10^3 \text{ s}^{-1}$.

3.2. Electrochemical confirmation of the interaction of MXF with DNA

CV and DPV of MXF in presence and absence of Hs-DNA are shown in Fig. 5 and Fig. 6 respectively.

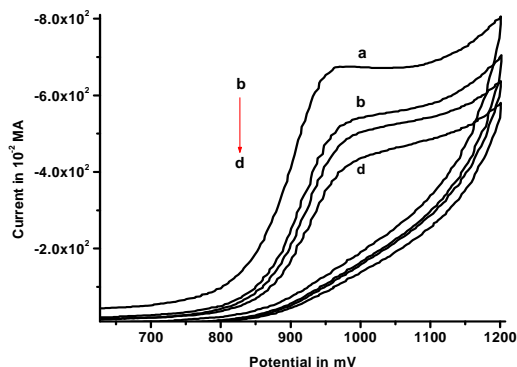


Fig 5: Cyclic voltammogram of a) 1.5×10^{-4} M MXF in the absence of DNA and the presence of $C_{DNA} = 5.0, 10.0, 15.0 \mu\text{M L}^{-1}$ BSA (b to d) in BR buffer of pH-7.0 at scan rate 50 mVs^{-1} .

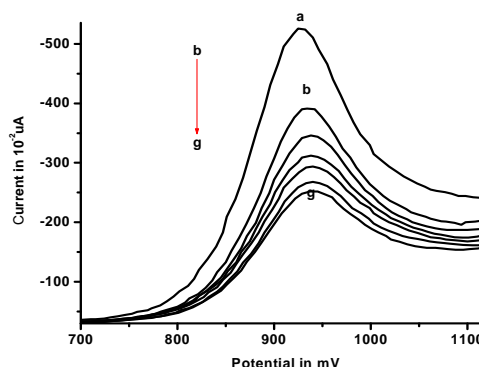


Fig 6: Differential pulse voltammogram of a) 1.5×10^{-4} M MXF in the absence of DNA and the presence of $C_{DNA} = 5.0, 10.0, 15.0, 20.0, 25.0, 30.0 \mu\text{M L}^{-1}$ BSA (b to d) in BR buffer of pH-7.4 at scan rate 50 mVs^{-1} .

MXF exhibited a single well defined anodic peak at 981 mV vs CPE in BR buffer (pH 7.4), which corresponds to the oxidation of the -N-H group [10]. Addition of DNA to MXF results in decrease of peak current of MXF. The decrease in peak current of MXF upon addition of DNA may be attributed to several possible reasons. The major electrochemical kinetic parameters (α and k_0) of MXF in presence and absence of DNA can demonstrate whether DNA influences the electrochemical kinetics of MXF or not. The values of α and k_0 are found to be 0.539 and 0.9849 s^{-1} in absence of DNA and 0.612 and $1.139 \times 10^3 \text{ s}^{-1}$ in presence of DNA. In this way, appreciable difference in the values of α and k_0 in presence and absence of DNA was not observed indicating that the DNA did not alter the electrochemical kinetics of MXF oxidation. The small negative shift observed in the oxidation potential of MXF may be evidence of electrostatic interactions [15].

The binding constant was calculated using following equation [16,17]:

$$\log \left(\frac{1}{[\text{DNA}]} \right) = \log K + \log \left(\frac{I}{I_0 - I} \right)$$

Where, K is the binding constant, I_0 and I are the anodic peak currents of free MXF and MXF-DNA complex, respectively. The plot of $\log (1/[\text{DNA}])$ vs $\log (I/(I_0 - I))$ constructed. From the ratio of the intercept to slope, K was estimated to be $9.384 \times 10^4 \text{ L mol}^{-1}$ and the correlation coefficient was found as 0.9965 ($n = 6$).

3.3. UV-vis Spectroscopic study

The interaction between MXF and Hs-DNA has been characterized classically by UV-vis absorption spectra. The MXF exhibits maximum absorbance at 289 nm in the range of 200 - 400 nm. The effect of progressive increasing concentration of Hs-DNA (5 to $15 \mu\text{M L}^{-1}$) on the absorption spectrum of MXF ($1.0 \times 10^{-4} \text{ M}$) is shown in Fig. 7 A. The absorption spectra show an increase of peak intensity about 22.4 % and a small red shift about 10 nm at absorption band of MXF with increasing concentration of Hs-DNA. The hypochromicity and bathochromicity of absorption band are due to the effective interaction between MXF with Hs-DNA. The results revealed that intercalation may be ruled out as a major binding mode of MXF with DNA. Therefore, we propose electrostatic binding mode between MXF and Hs-DNA based on variations in absorbance spectra of MXF upon binding to Hs-DNA. The binding constant (K), was calculated using the equation,

$$\frac{A_0}{A - A_0} = \frac{\epsilon_G}{\epsilon_{H-G} - \epsilon_G} + \frac{\epsilon_G}{\epsilon_{H-G} - \epsilon_G} \times \frac{1}{K[\text{DNA}]}$$

Where, A_0 and A are the absorbance of drug in the absence and presence of Hs-DNA, ϵ_G and ϵ_{H-G} are the absorption coefficients of drug and its complex with Hs-DNA, respectively. The plot of $A_0/(A - A_0)$ versus $1/[\text{DNA}]$ was constructed as shown in Fig. 7 B.

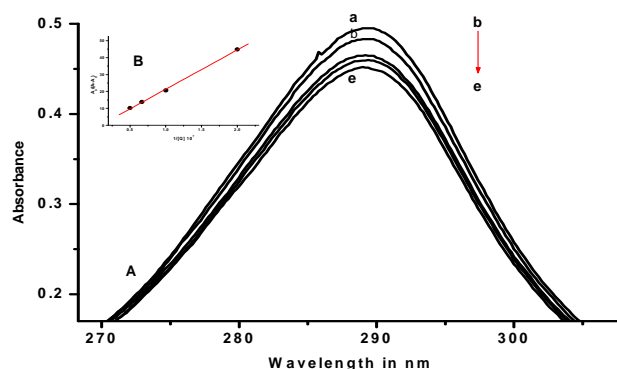


Fig 7 : (A) UV-visible spectra of (a) 1×10^{-4} M MXF in the absence of Hs-DNA and in presence of $C_{\text{DNA}} = 5, 10, 15 \mu\text{ML}^{-1}$ of HS-DNA (b to d) in BR buffer of pH 7.4; (B): Plot of $(A_0 / (A-A_0))$ vs. $1 / [\text{HS-DNA}]$

From the ratio of intercept to slope, the binding constant, K was estimated to be $4.2296 \times 10^5 \text{ L mol}^{-1}$ which is consistent with that reported value ($K \approx 10^3 - 10^5$) [9]. This indicates that MXF shows strong affinity with Hs-DNA (Lu et al. 2011). Standard free energy change, ΔG^0 (at 27°C) was evaluated from K using the relationship $\Delta G^0 = -2.303RT \log K$. It was found to be $-17.866 \text{ kJ mol}^{-1}$ indicating the spontaneity of the reaction.

3.4. Spectrofluorimetric study of MXF-HsDNA complex

A strong fluorescence emission spectrum of MXF at 503 nm was observed in the range of 350 - 550 nm after excitation at 289 nm. The fluorescence emission intensity of MXF increased with increasing concentration of Hs-DNA (Fig. 8A). An enhanced fluorescence intensity of MXF was observed with the increasing concentration of Hs-DNA, but not altering the emission maximum and shape of the peak. This is due to the microenvironment around the chromophore of MXF is changed which increases the molecular planarity of the complex and decreases the collision frequency of solvent molecules with MXF. This is due to diffusion which occurs between adjacent base pairs of Hs-DNA [19]. The fluorescence intensity tends to be constant at a high concentration of Hs-DNA, which shows the binding of MXF to Hs-DNA reached saturation.

The binding constant was calculated according to Stern-Volmer equation,

$$F_0 / F = 1 + k_q \tau_0 [Q] = 1 + K_{sv} [Q]$$

Where, F_0 and F are the fluorescence intensities in absence and presence of Hs-DNA respectively, $[Q]$ is the concentration of quencher, k_q is the quenching rate constant, τ_0 is the average life time of biomolecule without quencher and its value 10^{-8} s and K_{sv} is the Stern-volmer quenching constant. The values of K_{sv} and K_q can be determined from the slope of regression curve F_0/F vs $[Q]$ [Fig. 8 B].

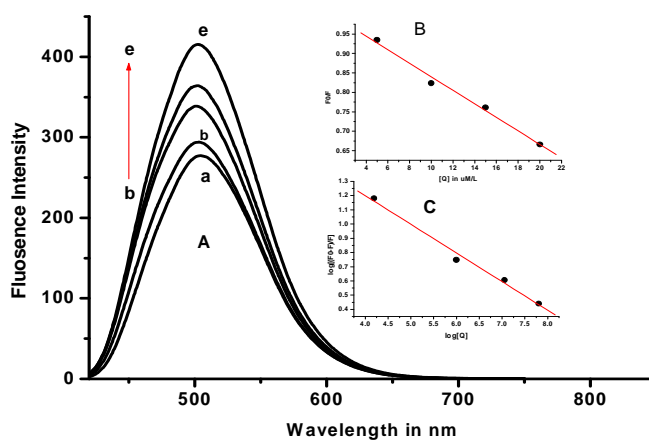


Fig 8 (A) Fluorescence spectra of (a) 1.5×10^{-4} M MXF in the absence of Hs-DNA and the presence of $C_{\text{DNA}} = 5.0, 10.0, 15.0, 20.0, 25.0, 30.0, 35.0 \mu\text{M L}^{-1}$ Hs-DNA (b to h) in BR buffer of pH-7.4; (B) Stern-volmer plot of (F / F_0) vs. $[Q]$ and (C) Plot of $\log [(F_0 - F)/F]$ vs. $\log [Q]$

The binding constant (K_{sv}) and K_q values calculated were $5.611 \times 10^5 \text{ L mol}^{-1}$ and $5.611 \times 10^{13} \text{ L mol}^{-1} \text{ s}^{-1}$ ($R^2 = 0.9988$) respectively. The maximum rate constant of collisional quenching (K_q) of various quenchers with biopolymers is about $2.0 \times 10^{10} \text{ L mol}^{-1} \text{ s}^{-1}$ [20], which suggests that the fluorescence quenching process may be mainly controlled by static quenching mechanism rather than dynamic. Standard free energy change, ΔG^0 (at 27°C) was evaluated from K using the relationship $\Delta G^0 = -2.303 RT \log K$. It was found to be $-21.369 \text{ k J mol}^{-1}$ indicating the spontaneity of the reaction.

3.5. Determination of binding constant and number of binding sites

The binding constant and number of binding sites for MXF-Hs-DNA were determined by the following equation [21].

Where, K_b and n are binding constant and number of binding sites respectively. The values of n and K_b can be determined from the slope and intercept of the double logarithm regression curve $\log [(F_0 - F)/F]$ versus $\log [Q]$ [Fig. 8C]. The value of K_b was found to be $4.964 \times 10^5 \text{ L mol}^{-1}$ ($R^2 = 0.9988$) and the value of n is ~ 2 . The n value indicates that there is one independent class of binding sites in Hs-DNA for MXF. Standard free energy change, ΔG^0 (at 27°C) evaluated from K using the relationship $\Delta G^0 = -2.303 RT \log K$ was found to be $-19.851 \text{ k J mol}^{-1}$ indicating the spontaneity of the reaction.

The binding constant and number of binding sites are also calculated according to the equation $\theta = (F_0 - F)/F_0$ [22]. Where, F and F_0 are the fluorescence intensities of MXF with and without DNA. Fluorescence data was analyzed using the method described by Ward [23].

$$\log \left[\frac{(F_0 - F)}{F} \right] = \log K_b + n \log [Q].$$

$$\frac{1}{(1 - \theta)K} = \frac{[D_t]}{\theta} - n[P_T]$$

Where, K is the association constant for drug-Hs-DNA interaction, n is the number of binding sites, $[D_t]$ is the total drug concentration and $[P_T]$ is the total Hs-DNA concentration. The values of n and K can be determined from the slope and intercept of the double logarithm regression $1/(1 - \theta)$ versus $\log [D_t]/\theta$ (Fig. 9). The values of K and n are found to be $5.3 \times 10^5 \text{ L mol}^{-1}$ and 2.03 respectively. Standard free energy change, ΔG^0 (at 27°C) was found to be $-20.663 \text{ k J mol}^{-1}$ indicates the reaction is spontaneous.

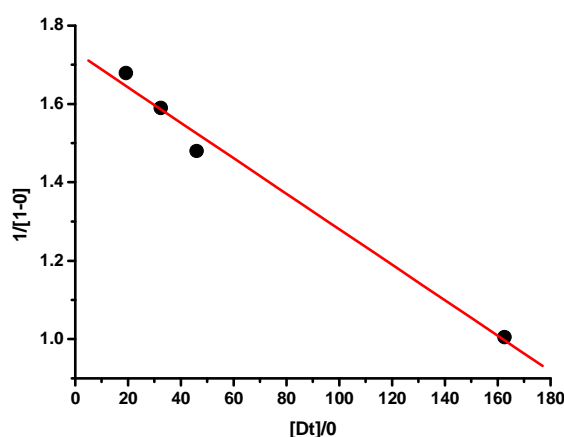


Fig 9: Plot of $1/(1 - \theta)$ vs. $[D_t]/\theta$ for MXF-Hs-DNA system

3.6. Viscometric study

Optical photophysical studies provide necessary but not sufficient clues to explain a binding between DNA and the complex, while hydrodynamic measurements that are sensitive to the length change are regarded as the least ambiguous tests of a binding model in solution [24]. Thus, viscosity measurements were carried out as an effective tool to further clarify the binding mode of MXF to Hs-DNA. An intercalator is generally known to cause a significant increase in the viscosity of DNA solution due to lengthen the DNA helix as base pairs are separated to accommodate the binding ligand [25]. In contrast, a partial, non-classical ligand intercalation in grooves causes a

bend in DNA helix reducing its effective length and thereby its viscosity [26]. As illustrated in Fig. 10, the relative viscosities of the Hs-DNA increased steadily upon the increasing concentration of MXF. Such behaviour further confirmed that MXF bound to DNA through a non-classical intercalation or groove mode via hydrophobic interaction.

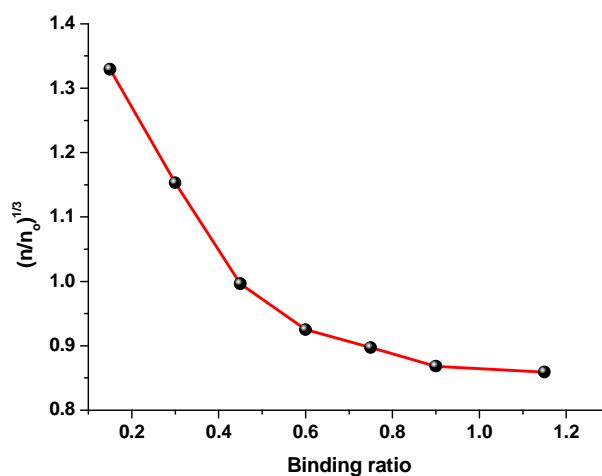


Fig 10: Effect of increasing concentration of Hs-DNA on the relative viscosity of MXF

CONCLUSION

The interaction between MXF and Hs-DNA was studied by different electrochemical, spectroscopic and viscometric methods at pH 7.4. In voltammetric studies, it was observed that the presence of DNA reduces the equilibrium concentration of free MXF and produces an electrochemically inactive complex. Both electrostatic interactions and minor groove binding modes were deduced from the results of different methods, although groove binding seemed to be predominant. Thermodynamic parameters like binding constant, changes in enthalpy and Gibbs free energy during the interaction process were calculated. The interaction was favourable with respect to both enthalpic and entropic changes, and the negative sign of Gibbs free energy change shows the spontaneity of interaction between MXF and Hs-DNA.

Acknowledgement

The authors are grateful for the financial support provided by the University Grants Commission, New Delhi, India (F. No. 42-308/2013 (SR) Dated, 28/03/2013). Thanks are also due to the Principal, Maharani's Science College for Women, Bangalore for providing necessary infrastructural facilities.

REFERENCES

- [1] Blondeau, J.M.; *Clin. Therm.* 21, (1999), 3-40.
- [2] Langlois, M.H.; Montagut, M.; Dubost, J.P.; Grellet, J.; Saux, M.C.; *J. Pharm. Biomed. Anal.* 37, (2005), 389-393.
- [3] Siefert, H.M.; Domdey-Bette, A.; Henninger, K.; Hucke, F.; Kohlsdorfer, C.; Stass, H.H.; *J. Antimicro. Chemother.*, 43, (1999), 69-76.
- [4] Stass, H.H.; Dalhoff, A.; Kubitzka, D.; Schuhly, U.; *Antimicro. Agents. Chemo.*, 42, (1998), 2060-2065.
- [5] Malathum, K.; Singh, K.V.; Murray, B.E. *Diagn. Microbiol. Infect. Dis.* 35, (1999), 127-133.
- [6] Soussy, C.J.; *Med. Mal. Infect.* 33, (2003), 125-133.
- [7] Zeglis, B.M.; Pierre, V.C.; Barton, J.K. *Chem. Commun.* 44, (2007), 4565-4579.
- [8] Laviron, E.; Roullier, L.; Degrand, C., *J. Electroanal. Chem.*, 112, (1980), 11-23.
- [9] Hammam, E., *J. Pharma and Biomed.*, 30, (2002), 651-659.
- [10] Teradal, N.L.; Prashanth, S.N.; Seetharamappa J., *Electrochem. Sci. Eng.* 2, (2012), 67-75.
- [11] Kalanur, S.S.; Seetharamappa, J.; *Anal. Lett.* 43, (2010), 618-630.
- [12] Bard, A.J.; Faulkner, L.R., Wiley, New York, (1980)
- [13] Laviron, E., *J. Electroanal. Chem.* 52, (1974), 355-393.
- [14] Laviron, E., *J. Electroanal. Chem.* 101, (1979), 19-28.
- [15] Li, N.; Ma, Y.; Yang, C.; Guo, L.; Yan, X. *Biophys. Chem.* 116, (2005), 199-205.
- [16] Feng, Q.; Li, N.Q.; Jiang, Y.Y. *Anal. Chim. Acta* 344, (1997), 97-104.
- [17] Fahimeh, J.; Parisa, S. Dorraji, *J. Pharm. and Biomed. Anal.* 70, (2012), 598-601

- [18] Lu, Y.; Gong-Ke W.; Lv, J.; Gui-Sheng, Z.; Quing-Feng L., *J. Fluoresc.* 21, (2011) 9409 – 414
- [19] Hajian R.; Zafari, M., *Chin. J. Chemistry*, 29, (2011), 353-1358.
- [20] Taniou, F.A.; Ding, D.Y.; Patrick, D.A.; Tidwell, R.R.; Wilson, W.D.; *Biochem.*, 36, (1997) 15315.
- [21] Chuanxian Wang; Qinghua Chu; Changyun Chen, Zhao Bo, 25, (2011), 113-122.
- [22] Weber, G.; Young, L.B., *J. Biol. Chem.* 239, (1964), 1415-1419.
- [23] Ward, L.D.; *Methods in Enzymology.*, 17, (1985), 400-404.
- [24] Streckowski, L.; Wilson, B., *Mutation Research*, 623, (2007) 3-13.
- [25] Li, Y.P.; Yang, P., *Chin. J. Chem.*, 28, (2010), 759-765.
- [26] Zhao, N.; Wang, X.M.; Pan, H.Z.; Hu, Y.M.; Ding, L.S., *Spect. Chim. Acta, Part A* 75, (2010), 1435–1442.